

4-(1,2,4-三唑-1-基)苯酚铜(II)/镍(II)配合物的晶体结构及荧光性质

赵红昆 丁 波 王修光 贾 芳 杨恩翠* 赵小军*

(天津师范大学化学学院,无机-有机杂化功能材料化学教育部重点实验室,
天津市功能分子结构与性能重点实验室,天津 300387)

摘要: 合成并通过单晶和粉末 X 射线衍射、元素分析、红外光谱、热失重以及荧光光谱技术表征了含有 4-(1,2,4-三唑-1-基)苯酚(hptrz)配体的 2 个过渡金属配合物 $[\text{Ni}(\text{H}_2\text{O})_2(\text{hptrz})_2(\text{tp})] \cdot 2\text{DMF}_n$ (**1**)和 $[\text{Cu}(\text{hptrz})_2(\text{SCN})_2] \cdot 2\text{H}_2\text{O}$ (**2**)(H₂tp 为对苯二甲酸)。配合物 **1** 中八面体的 Ni(II)离子由 tp²⁻阴离子拓展形成线性的一维链状结构;而配合物 **2** 则呈现中心对称的单核结构。配合物中,中性的 hptrz 配体呈现端基配位模式,并通过形成 O-H...O 氢键相互作用将低维结构拓展为高维超分子网络。此外,配体内的电荷转移使这 2 个配合物均在紫外区发射出强的荧光发射峰。

关键词: 4-(1,2,4-三唑-1-基)苯酚;铜(II)/镍(II)配合物;晶体结构;荧光性质

中图分类号: O614.121; O614.81+3

文献标识码: A

文章编号: 1001-4861(2018)09-1739-08

DOI:10.11862/CJIC.2018.219

Crystal Structures and Fluorescence Properties of Cu(II)/Ni(II) Complexes with 4-(1,2,4-Triazol-1-yl)phenol Ligand

ZHAO Hong-Kun DING Bo WANG Xiu-Guang JIA Fang YANG En-Cui* ZHAO Xiao-Jun*

(College of Chemistry, Key Laboratory of Inorganic-Organic Hybrid Functional Material Chemistry,
Ministry of Education, Tianjin Key Laboratory of Structure and Performance for
Functional Molecules, Tianjin Normal University, Tianjin 300387, China)

Abstract: Two 4-(1,2,4-triazol-1-yl)phenol (hptrz)-based transition metal complexes, $[\text{Ni}(\text{H}_2\text{O})_2(\text{hptrz})_2(\text{tp})] \cdot 2\text{DMF}_n$ (**1**) and $[\text{Cu}(\text{hptrz})_2(\text{SCN})_2] \cdot 2\text{H}_2\text{O}$ (**2**) (H₂tp=terephthalic acid), have been prepared and characterized by single-crystal and powder X-ray diffractions, elemental analysis, FT-IR spectra, thermogravimetric and luminescence spectra. X-ray diffraction analysis revealed that **1** is a one-dimensional linear chain with octahedral Ni(II) ions extended by bis-unidentate tp²⁻ anions; whereas **2** exhibits a centrosymmetric mononuclear entity. The neutral hptrz ligand in the both complexes serves as terminal ligands to complete the metal coordination sphere and to help to assemble the low-dimensional aggregates into a high-dimensional supramolecular architecture by O-H...O hydrogen-bonding interactions. Additionally, the complexes display strong emissions in UV region originated from intraligand electronic transfer. CCDC: 746903, **1**; 746904, **2**.

Keywords: 4-(1,2,4-triazol-1-yl)phenol; Cu(II)/Ni(II) complexes; crystal structure; luminescent property

Transition metal complexes constructed from inorganic metal ions and various organic ligands have

attracted intense interest during the past decades, which is mainly attributed to their tailorable structures

收稿日期:2018-05-01。收修改稿日期:2018-06-22。

国家自然科学基金(No.21671149)和天津市高等学校创新团队培养计划(No.TD13-5074)资助项目。

*通信联系人。E-mail: encui_yang@163.com, xiaojun_zhao15@163.com

and promising properties in different fields^[1-7]. The successful preparations of the extended complexes with 1,2,4-triazole (Htrz) and its derivatives ligands have gained attractively considerable attention due to their novel framework topologies^[8-10] and potential applications in gas storage and luminescence properties^[11-15]. Compared with the unsubstituted triazoles, 4-(1,2,4-triazol-1-yl)phenol (hptrz) loses an active coordination site on the 1-positioned nitrogen due to the substitution of the H atom by a phenolic moiety, and can usually act as a terminal ligand to coordinate with the discrete metal ion in an unidentate mode. Therefore, the constructions of the extended structures with hptrz bridge are difficult and still challenging. Fortunately, hptrz-based Cd(II) coordination polymers with aromatic polycarboxylate coligands have been previously reported, which present strong hptrz-based fluorescence emissions^[20]. To the best of our knowledge, there exist few papers about Cu(II)/Ni(II)-polymers based on hptrz, *m*-phenol-1,2,4-triazole (*m*-ptz) or *p*-phenol-1,2,4-triazole (*p*-ptr) ligands with NCS anion^[16-17]. As part of our continuing investigations on coordination chemistry and photophysically properties of 1,2,4-triazole^[18-19] and its derivatives^[20-21], herein, hptrz and aromatic polycarboxylate and ammonium thiocyanate co-ligands were selected as mixed ligands to carry out the self-assembly reactions with Cu(II)/Ni(II) salts under controllable hydrothermal conditions. As a result, two crystalline transition metal complexes, $[\text{Ni}(\text{H}_2\text{O})_2(\text{hptrz})_2(\text{tp})] \cdot 2\text{DMF}$ (**1**) and $[\text{Cu}(\text{hptrz})_2(\text{SCN})_2] \cdot 2\text{H}_2\text{O}$ (**2**), were successfully isolated and structurally characterized. Structural determinations reveal that the different crystal structures of the two complexes with 1D polymeric chain for **1** and mononuclear structure for **2** are significantly governed by the co-ligands (aromatic carboxylate group vs ammonium thiocyanate). Acting as a terminal ligand, the neutral hptrz ligand binds with the central M(II) ion in terminally monodentate mode through triazolyl N donor, which is the common coordination mode of 1,2,4-triazole and its derivatives. Additionally, the luminescence behavior and thermal stability of the two resultant complexes are discussed in more details.

1 Experimental

1.1 Materials and physical measurements

All of the starting materials employed were commercially purchased (H₂tp was purchased from Acros and other commercially analytical-grade reagents were from Tianjin Chemical Reagent Factory) and used as received without further purification. Doubly deionized water was used for the conventional synthesis. Elemental analyses for C, H and N were performed on a CE-440 (Leeman-Labs) analyzer. Fourier transform (FT) IR spectra (KBr pellets) were taken on an Avatar-370 (Nicolet) spectrometer in the range of 4 000~400 cm⁻¹. Thermogravimetric analysis (TGA) experiments were carried out on Shimadzu simultaneous DTG-60A compositional analysis instrument from room temperature to 800 °C under N₂ atmosphere at a heating rate of 5 °C · min⁻¹. Fluorescence spectra of the polycrystalline powder samples were performed on a Cary Eclipse fluorescence spectrophotometer (Varian) equipped with a xenon lamp and quartz carrier at room temperature.

1.2 Synthesis of $[\text{Ni}(\text{H}_2\text{O})_2(\text{hptrz})_2(\text{tp})] \cdot 2\text{DMF}$ (**1**)

To a mixed DMF-methanol (1:1, V/V) solution (5.0 mL) containing hptrz (16.1 mg, 0.1 mmol) and H₂tp (16.6 mg, 0.1 mmol) was slowly added an aqueous solution (5.0 mL) of Ni(NO₃)₂ · 6H₂O (29.0 mg, 0.1 mmol) with constant stirring. The pH value of the resulting mixture was adjusted to 7 by triethylamine. Then, the mixture was further stirred for half hour and filtered. Blue block-shaped crystals suitable for X-ray diffraction were grown by slow evaporation of the filtrate within five days. Yield: 30% based on hptrz ligand. Anal. Calcd. for C₁₅H₁₈N₄Ni_{0.50}O₅ (%): C: 49.54; H: 4.99; N: 15.41. Found (%): C: 49.03; H: 4.56; N: 15.98. FT-IR (cm⁻¹, pellet): 3 434br, 1 659s, 1 562s, 1 525s, 1 439w, 1 385s, 1 279m, 1 246w, 1 145w, 834m, 752m, 667m, 629m.

1.3 Synthesis of $[\text{Cu}(\text{hptrz})_2(\text{SCN})_2] \cdot 2\text{H}_2\text{O}$ (**2**)

To a methanol solution (5.0 mL) containing hptrz (16.1 mg, 0.1 mmol) and NH₄SCN (15.2 mg, 0.2 mmol) was slowly added to an aqueous solution (5.0 mL) of

$\text{Cu}(\text{OAc})_2 \cdot \text{H}_2\text{O}$ (19.9 mg, 0.1 mmol). The resulting mixture was further stirred vigorously for ca. 30 min and filtered. Green block-shaped crystals suitable for X-ray diffraction were obtained by slow evaporation of the filtrate in five days. Yield: 45% based on hptrz ligand. Anal. Calcd. for $\text{C}_{18}\text{H}_{18}\text{CuN}_4\text{O}_5\text{S}_2$ (%): C: 40.18; H: 3.37; N: 20.83. Found (%): C: 39.86; H: 3.02; N: 21.37. FT-IR (cm^{-1} , pellet): 3 464br, 2 099vs, 1 600m, 1 525s, 1 485w, 1 438w, 1 358w, 1 280m, 1 222w, 1 144m, 1 055w, 980w, 837m, 671w, 641w, 468w.

1.4 X-ray crystallography

Diffraction intensities for **1** and **2** were collected on a Bruker APEX II CCD diffractometer equipped with graphite-monochromated $\text{Mo } K\alpha$ radiation with radiation wavelength of 0.071 073 nm by using a ω - φ scan technique at 296(2) K. There was no evidence of crystal decay during the data collection process. The

program SAINT^[22] was used for integration of the diffraction profiles. Semi-empirical absorption corrections were applied using SADABS program^[23]. The structures were solved by direct methods and refined with the full-matrix least-squares technique using the SHELXS-97 and SHELXL-97 programs^[24]. Anisotropic thermal parameters were assigned to all non-hydrogen atoms. The H atoms of the water molecules except for the splitting water were located from difference maps and refined with isotropic temperature factors. No attempts have been performed to locate hydrogen atoms of the splitting water molecules. The crystallographic data and experimental details for structural analyses are summarized in Table 1. Selected bond distances and angles are listed in Table 2. Hydrogen bond geometries are given in Table 3.

CCDC: 746903, **1**; 746904, **2**.

Table 1 Crystal data and structure refinement for **1** and **2**

	1	2
Formula	$\text{C}_{15}\text{H}_{18}\text{N}_4\text{Ni}_2\text{O}_5$	$\text{C}_9\text{H}_9\text{Cu}_{0.5}\text{N}_4\text{O}_2\text{S}$
Formula weight	363.69	269.03
Size / mm	0.24×0.21×0.18	0.25×0.23×0.20
Crystal system	Triclinic	Monoclinic
Space group	$P\bar{1}$	$P2_1/c$
a / nm	0.698 95(15)	0.549 31(4)
b / nm	1.134 4(2)	1.661 63(13)
c / nm	1.206 7(3)	1.189 59(9)
α / (°)	109.849(2)	
β / (°)	97.567(2)	91.000 0(10)
γ / (°)	99.180(2)	
V / nm^3	0.870 4(3)	1.085 6(31)
Z	2	4
θ range / (°)	1.96~25.00	2.11~25.01
Index ranges	$-7 \leq h \leq 8, -12 \leq k \leq 13, -14 \leq l \leq 10$	$-6 \leq h \leq 6, -19 \leq k \leq 17, -14 \leq l \leq 11$
D_c / ($\text{g} \cdot \text{cm}^{-3}$)	1.388	1.646
μ / mm^{-1}	0.623	1.243
Reflection collected, Unique	4 740, 3 028	5 829, 1 917
R_{int}	0.011 5	0.017 1
GOF	1.032	1.044
$F(000)$	380	550
R_1^a, wR_2^b [$I > 2\sigma(I)$]	0.028 3, 0.076 3	0.023 3, 0.066 3
R_1, wR_2^b (all data)	0.030 3, 0.077 4	0.026 6, 0.068 2
Largest diff. peak and hole / ($\text{e} \cdot \text{nm}^{-3}$)	284, -275	267, -253

^a $R_1 = \sum \|F_o| - |F_c|\| / \sum |F_o|$; ^b $wR_2 = [\sum w(F_o^2 - F_c^2)^2 / \sum w(F_o^2)]^{1/2}$.

Table 2 Selected bond lengths (nm) and angles (°) for **1** and **2**

1					
Ni(1)-O(3)	0.204 23(12)	Ni(1)-O(5W) ⁱ	0.206 92(12)	Ni(1)-N(3)	0.209 97(15)
O(3)-Ni(1)-N(3)	87.36(5)	O(5W)-Ni(1)-N(3)	93.10(5)	O(3)-Ni(1)-O(5W)	86.67(5)
O(5W) ⁱ -Ni(1)-N(3)	86.90(5)	O(3)-Ni(1)-O(5W)	93.33(5)	O(3)-Ni(1)-N(3) ⁱ	92.64(5)
O(3) ⁱ -Ni(1)-O(5W) ⁱ	86.67(5)	O(5W) ⁱ -Ni(1)-N(3) ⁱ	93.10(5)		
2					
Cu(1)-N(4)	0.195 43(15)	Cu(1)-N(3)	0.202 04(15)		
N(4)-Cu(1)-N(3)	90.11(6)	N(4)-Cu(1)-N(3) ⁱ	89.89(6)		

Symmetry codes: ⁱ 1-x, 1-y, 1-z for **1**; ⁱ 1-x, 1-y, 1-z for **2**.**Table 3** Hydrogen-bonding parameters for **1** and **2**

D-H...A	d(D-H) / nm	d(H...A) / nm	d(D...A) / nm	D-H...A / (°)
1				
O1-H1...O4 ⁱⁱ	0.082	0.182	0.264 1(2)	175
O5W-H5A...O4	0.083	0.192	0.270 1(4)	155
O5W-H5B...O6 ⁱⁱⁱ	0.084	0.198	0.278 5(9)	160
2				
O1-H1...O2 ^{iv}	0.082	0.198	0.279 4(7)	174
O2-H2A...S1 ⁱⁱⁱ	0.085	0.269	0.349 0(0)	158
O2-H2B...S1 ^{iv}	0.085	0.279	0.360 0(4)	161

Symmetry codes: ⁱⁱ x, y, z-1; ⁱⁱⁱ x-1, y, z for **1**; ⁱⁱⁱ x-1, y, z; ^{iv} x+1, 1/2-y, z-1/2 for **2**.

2 Results and discussion

2.1 Synthesis

Complexes **1** and **2** were successfully obtained as crystalline products by conventional evaporation method. Complex **1** was isolated in mixed methanol-DMF and the pH value of the resulting mixture was adjusted to 7.0 by triethylamine, while **2** was generated in mixed methanol-water solution without control the pH value. The lattice solvent molecule of **1** was slightly different from those in **2**. Thus, it can be concluded that the reaction medium is highly important for preparation of the target crystalline samples.

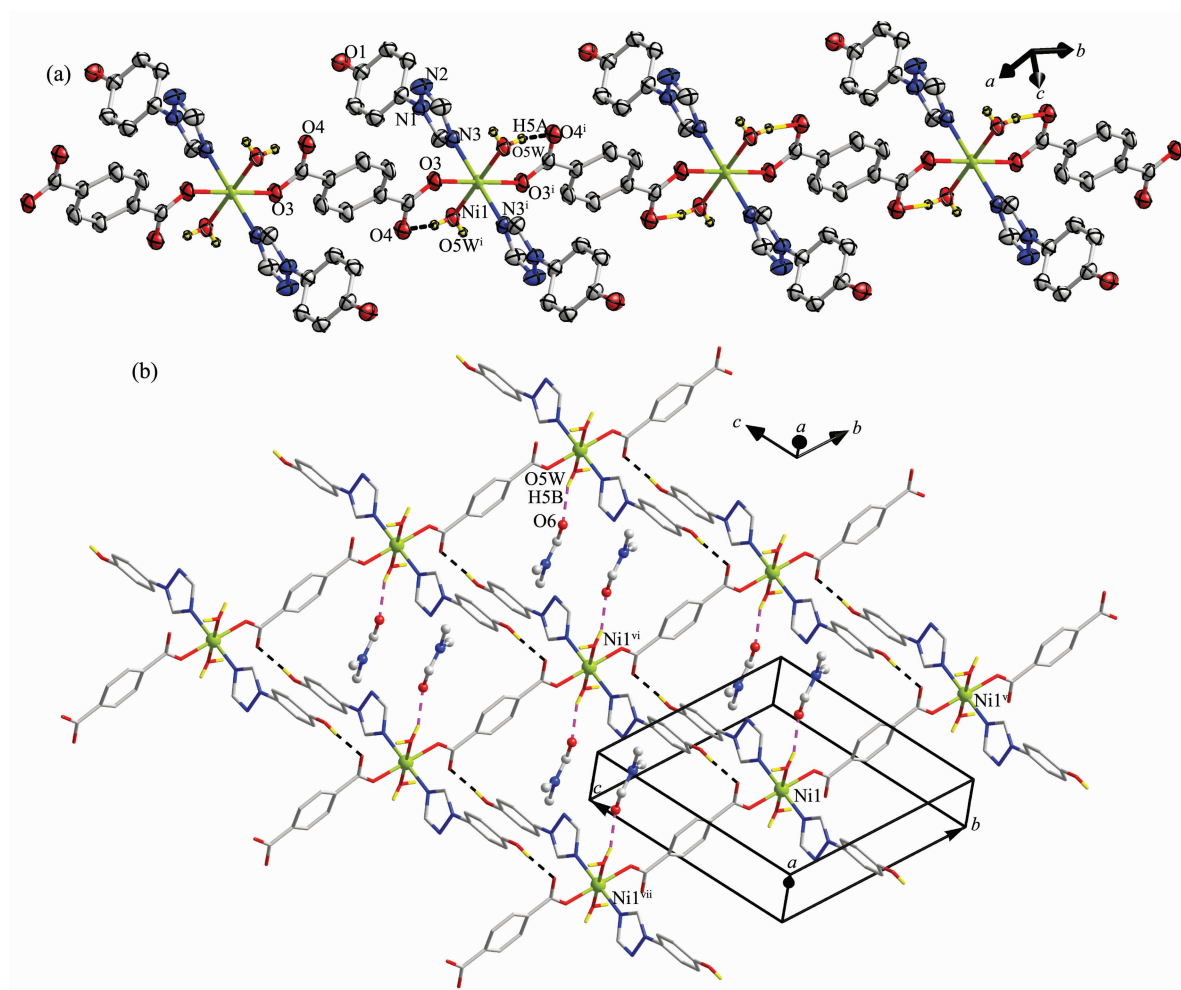
2.2 Descriptions of crystal structures

Single crystal X-ray diffraction reveals that complex **1** crystallizes in the $P\bar{1}$ space group, consisting of a polymeric one-dimensional (1D) chain with slightly distorted Ni(II) octahedra bridged by doubly deprotonated tp^{2-} anions. The asymmetric unit of **1** contains one hexa-coordinated Ni(II) ion, two neutral

hptrz ligands, two terminally coordinated water molecules, one doubly deprotonated tp^{2-} dianion and two lattice DMF molecules.

As shown in Fig.1a, the crystallographically unique Ni(II) ion in **1** is six-coordinated by two triazolyl N atoms from two distinct hptrz ligands in the axial sites, and four O atoms from two carboxylate groups of two *trans*-bound tp^{2-} anions and two water molecules in the equatorial plane, adopting an axially elongated octahedral geometry with the axial Ni-N distances slightly longer by than those of Ni-O bonds in the equatorial plane (Table 2).

The fully deprotonated tp^{2-} anions bridge the adjacent Ni(II) ions in a bis-unidentate binding fashion, leading to a 1D linear chain running along the crystallographic *b*-axis. The intrachain Ni(II) ... Ni(II) distance is 1.134 4(2) nm separated by tp^{2-} anion. Additionally, there exist pairs of intrachain O-H...O hydrogen-bonding interactions between coordinated water molecule and carboxylate O donor of tp^{2-} dianion,



Only hydrogen atoms involved in water molecular were included; Symmetry codes: ⁱ $1-x, 1-y, 1-z$ in (a);
^v $x, 1+y, z$, ^{vi} $x, y, 1+z$, ^{vii} $x, y-1, z$ in (b)

Fig.1 Crystal structure of **1**: (a) Polymeric 1D chain of **1** with atomic labels in the asymmetric unit showing 60% probability displacement ellipsoids; (b) 2D supramolecular sheet of **1** with lattice DMF molecules encapsulated in the grids

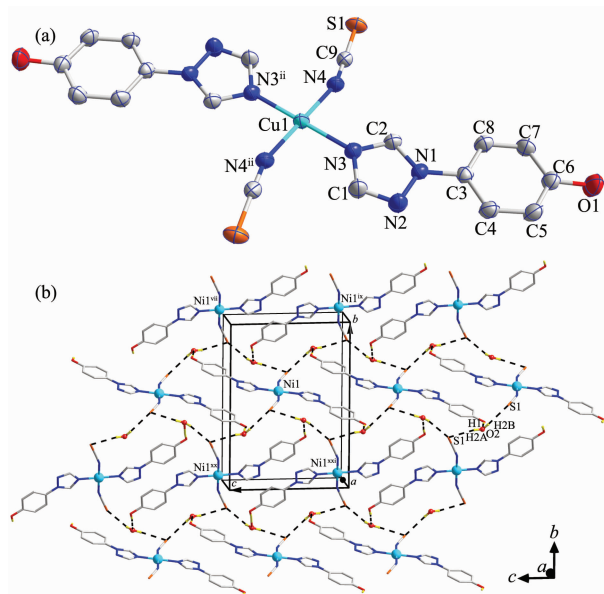
which help to consolidate the 1D chain structure of **1** (Fig.1b).

In addition to presenting the triazolyl N donor to coordinate with the Ni (II) atom in a commonly observed monodentate mode, the neutral hptrz ligand can also provide the uncoordinated phenolic OH group as a hydrogen-bond donor to produce interchain O—H \cdots O H-bonding interaction with the carboxylate group of tp^{2-} dianion from the adjacent chain, which assemble the 1D chains into a supramolecular 2D grid-based layer (Fig.1b and Table 3). Two lattice DMF molecules are encapsulated in the grids through O—H \cdots O hydrogen-bonding interactions.

Complex **2** exhibits a centrosymmetric mononu-

clear structure, similar to that of $[\text{Cu}(\text{C}_2\text{N}_3)_2(\text{C}_8\text{H}_7\text{N}_3\text{O})_2]$ reported previously^[21e]. As shown in Fig.2a, the sole Cu(II) atom in **2** is coordinated to four N atoms, in which two N donors are from two symmetry-related neutral hptrz and the others belong to a pair of isothiocyanate anions. The *cis* N—Cu—N bond angles are $89.89(6)^\circ$ and $90.11(6)^\circ$, respectively, indicating a slightly distorted square planar environment. Possessing potentially versatile binding modes with different metal ions^[25], the isothiocyanate anion herein acts simply as a terminal ligand to coordinate with Cu(II) center through nitrogen atom with the separations of Cu—N of 0.195 43(15) nm, which is shorter by 0.007 nm than that of Cu—N_{hptrz} (Table 2). The different bond

lengths indicates the variable binding strength of the two mixed ligands upon coordinating with the Cu(II) ion, which can influence the compositional stability of the resulting complex. Thus, the lattice water molecules play important roles for the periodic arrangement of the mononuclear entity, in which two types of hydrogen-bonding interactions ($\text{O}-\text{H}\cdots\text{O}$ and $\text{O}-\text{H}\cdots\text{S}$) involved the lattice water molecule were observed (Fig.2b). On one hand, lattice water molecule acts as H-bond acceptor, producing $\text{O}-\text{H}\cdots\text{O}$ H-bonding interaction with phenolic group formed with donor-acceptor distance of 0.279 4(7) nm. On the other hand, water molecule can also participate two $\text{O}-\text{H}\cdots\text{S}$ H-bonding interactions with two isothiocyanate anions with $\text{O}\cdots\text{S}$ distances of 0.349 0(0) and 0.360 0(4) nm, respectively. Thus, acting as a triple bridge, the lattice water molecules link the $[\text{Cu}(\text{hptrz})_2(\text{SCN})_2]$ units into a 2D wave-like layer in the crystallographic bc plane, and the nearest nonbonding $\text{Cu}(\text{II})\cdots\text{Cu}(\text{II})$ distances are 1.021 7(8) nm and 1.189 5(9) nm along b and c directions.



Hydrogen atoms were omitted for clarity; Symmetry codes: ⁱⁱ $x, y, z-1$ in (a); ^{vii} $2-x, 0.5+y, 1.5-z$, ^{ix} $2-x, 0.5+y, 0.5-z$, ^{ix} $2-x, y-0.5, 1.5-z$, ^{xii} $2-x, y-0.5, 0.5-z$ in (b)

Fig.2 (a) Mononuclear structure of **2** showing 60% probability displacement ellipsoids; (b) 2D layer of **2** formed by hydrogen-bonding interactions between mononuclear entities and lattice water molecules

2.3 IR spectra

In FT-IR spectra, the broad and strong absorption band appeared at $3\,434\text{ cm}^{-1}$ for **1** and $3\,464\text{ cm}^{-1}$ for **2** should be respectively ascribed to stretching vibration of the O-H, confirming the presence of water and phenolic group of hptrz ligand. The medium bands appeared at $800\sim 1\,400\text{ cm}^{-1}$ in both **1** and **2** should be associated with triazole ring vibrations of hptrz ligand^[26,34]. The absence of the band at $1\,681\text{ cm}^{-1}$ in **1** suggests the full deprotonation of H_2tp ligands^[26]. Strong characteristic bands for the asymmetric ($1\,659$ and $1\,562\text{ cm}^{-1}$) and symmetric stretching vibrations ($1\,439$ and $1\,385\text{ cm}^{-1}$) of the carboxylate group can be observed in the spectrum of **1**. For **2**, the very strong band centering at $2\,099\text{ cm}^{-1}$ and the weak band locating at 468 cm^{-1} correspond to the N-bonded terminal isothiocyanate groups^[27]. Thus, the results of FT-IR spectra are in well agreement with those of crystal structure determinations.

2.4 Thermal analysis

To investigate the contribution of the co-ligand on the thermal stability of the resultant complexes, the thermogravimetric study of the complexes **1** and **2** were performed at an inert atmosphere from room temperature to $800\text{ }^\circ\text{C}$ (Fig.3). Complex **1** can be thermally stable below $108\text{ }^\circ\text{C}$ and was followed by an obvious weight-loss stage between 108 and $426\text{ }^\circ\text{C}$. Once the temperature was beyond $426\text{ }^\circ\text{C}$, the decomposition of **1** finished completely, leaving NiO as final residue (Obsd. 9.9%, Calcd. 10.3%). The first weight-loss stage of **2** was between 107 and $139\text{ }^\circ\text{C}$, corresponding to the loss of lattice water molecules (Obsd. 7.0%, Calcd. 6.7%). Owing to the decomposition of

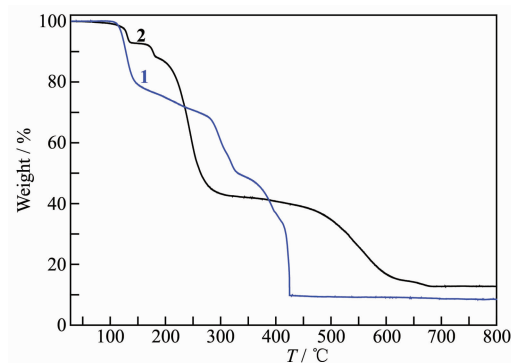


Fig.3 TGA curves for **1** and **2**

hptrz and SCN ligands, the mononuclear entity of **2** began to decompose at 163 °C, leaving CuO as final residue beyond 678 °C (Obsd. 14.0%, Calcd. 14.8%).

2.5 Fluorescent emissions

Fluorescent emission spectra of **1** and **2** in aqueous solution were measured at room temperature. As presented in Fig.4, the complexes displayed similar broad emissions centered at 422 nm upon excitation at 370 nm. To understand the nature of the charge transition, the luminescence properties of the free hptrz ligand under the same measurement conditions was also recorded for comparison. As a result, the neutral hptrz ligand displays a relatively strong emission band centered at 421 nm. Thus, the analogous emissions between hptrz and the complexes indicated that the emission were originate from π - π^* transfer of the core hptrz ligand, which is also similar with many fluorescent complexes based on the fluorescent ligands^[10].

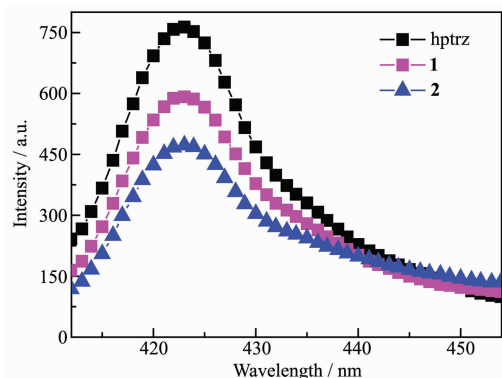


Fig.4 Fluorescence emission spectra of **1**, **2** and free hptrz in aqueous solution measured at room temperature

3 Conclusions

In summary, two new hptrz-based metal complexes were obtained by varying the transition metal ions and different co-ligands, exhibiting slightly bent 1D chain with slightly distorted Ni(II) octahedra extended by ditopic benzene-1,4-dicarboxylate connectors (**1**) and centrosymmetric mononuclear structure (**2**). Their structural difference is significantly directed by the tp^{2-} and SCN^- anion, rather than the terminal hptrz ligand. Owing to hptrz-based intraligand charge transfer, the two complexes show similar fluorescent emissions at

room temperature. Thus, the high stability and strong emission of the two target complexes in the solid state firmly ensure their potential applications as fluorescent materials.

Supporting information is available at <http://www.wjhxsb.cn>

References:

- [1] Rojas S, Carmona F J, Maldonado C R, et al. *Inorg. Chem.*, **2016**,55:2650-2663
- [2] He H M, Sun F X, Ma S Q, et al. *Inorg. Chem.*, **2016**,55: 9071-9076
- [3] WU Xiao-Shuo(吴小说), WANG Peng-Fei(汪鹏飞), LU Peng-Peng(路朋朋), et al. *Chinese J. Inorg. Chem.*(无机化学学报), **2016**,32(9):1667-1675
- [4] ZHANG Mei-Na(张美娜), ZHENG Xiao-Li(郑晓丽), QU Xiang-Long(屈相龙), et al. *Chinese J. Inorg. Chem.*(无机化学学报), **2017**,33(7):1172-1180
- [5] Bloch E D, Murray L J, Queen W L, et al. *J. Am. Chem. Soc.*, **2011**,133:14814-14822
- [6] WANG Li(王莉), KANG Quan-Peng(康全鹏), HAO Jing(郝静), et al. *Chinese J. Inorg. Chem.*(无机化学学报), **2018**,34(3):525-533
- [7] CHEN Jin-Wei(陈金伟), WEN Bing-Song(温炳松), CAO Fang-Li(曹芳利), et al. *Chinese J. Inorg. Chem.*(无机化学学报), **2017**,33(12):2322-2328
- [8] Ding B, Yi L, Gao H L, et al. *Inorg. Chem. Commun.*, **2005**, 8:102-104
- [9] Zhang J P, Chen X M. *Chem. Commun.*, **2006**,16:1689-1699
- [10] Zhai Q G, Lu C Z, Wu X Y, et al. *Cryst. Growth Des.*, **2007**, 7:2332-2342
- [11] Ouellette W, Hudson B S, Zubieta J. *Inorg. Chem.*, **2007**,46: 4887-4904
- [12] Haasnoot J G. *Coord. Chem. Rev.*, **2000**,200-202:131-185
- [13] Klingale M H, Brooker S. *Coord. Chem. Rev.*, **2003**,241:119-132
- [14] Beckman U, Brooker S. *Coord. Chem. Rev.*, **2003**,245:17-19
- [15] Abramovitch R A, Beckert J M, Gibson H H, et al. *J. Org. Chem.*, **2001**,66:1242-1251
- [16] Lavrenova L G, Ikorskii V N, Sheludyakova L A, et al. *Russ. J. Coord. Chem.*, **2004**,30:413-418
- [17] (a)Engelfriet D W, Verschoor G C, Den Brinker W. *Acta Crystallogr. Sect. B: Struct. Sci.*, **1980**,B35:1554-1560
(b)Yi L, Du J Y, Liu S, et al. *J. Chem. Res.*, **2004**,1:29-31
- [18] Yang E C, Liu Z Y, Wang X G, et al. *CrystEngComm*, **2008**,

- 10**:1140-1143
- [19](a)Liu Z Y, Wang X G, Yang E C, et al. *Z. Anorg. Allg. Chem.*, **2008**,**634**:1807-1811
- (b)Yang E C, Liang Q Q, Wang X G, et al. *Aust. J. Chem.*, **2008**,**61**:813-820
- [20]Yang E C, Jia F, Wang X G, et al. *Bull. Korean Chem. Soc.*, **2008**,**29**:2195-2201
- [21](a)Feng W, Chang R N, Wang J Y, et al. *J. Coord. Chem.*, **2010**,**63**:250-262
- (b)Yang E C, Feng W, Wang J Y, et al. *Inorg. Chim. Acta*, **2010**,**363**:308-316
- (c)Yang E C, Liu T Y, Wang Q, et al. *Inorg. Chem. Commun.*, **2011**,**14**:285-287
- (d)Yang E C, Yang Y L, Liu Z Y, et al. *CrystEngComm*, **2011**,**13**:2667-2673
- (e)Jia F, Li J, Wang X G, et al. *Acta Crystallogr. Sect. E: Struct. Rep. Online*, **2007**,**E63**:m31-m33
- [22]*SAINT Software Reference Manual*, Bruker AXS, Madison, WI, **1998**.
- [23]Sheldrick G M. *SADABS: Program for Empirical Absorption Correction of Area Detector Data*, University of Göttingen, Germany, **1996**.
- [24]Sheldrick, G M. *Acta Crystallogr. Sect. C: Cryst. Struct. Commun.*, **2015**,**C71**:3-8
- [25]Zhang H, Wang X M, Zhang K C, et al. *Coord. Chem. Rev.*, **1999**,**183**:157-195
- [26]Deacon G B, Phillips R J. *Coord. Chem. Rev.*, **1980**,**33**:227-250
- [27]Groeneveld L R, Vos G, Verschoor G C, et al. *J. Chem. Soc. Chem. Commun.*, **1982**:620-621